J Fluoresc (2013) 23:921–927
DOI 10.1007/s10895-013-1217-7

ORIGINAL PAPER

Interaction Mechanism of Trp-Arg Dipeptide with Calf Thymus DNA

Jing Lin · Canzhu Gao · Rutao Liu

Received: 8 November 2012 / Accepted: 1 April 2013 / Published online: 20 April 2013

Abstract The interaction between Trp-Arg dipetide (WR) and calf thymus DNA (ctDNA) in pH 7.4 Tris-HCl buffer was investigated by multi-spectroscopic techniques and molecular modeling. The fluorescence spectroscopy and UV absorption spectroscopy indicated that WR interacted with ctDNA in a minor groove binding mode and the binding constant was 4.1×10^3. The ionic strength effect and single-stranded DNA (ssDNA) quenching effect further verified the minor groove binding mode. Circular dichroism spectroscopy (CD) was employed to measure the conformation change of ctDNA in the presence of WR. The molecular modeling results illustrated that electrostatic interaction and groove binding coexisted between them and the hydrogen bond and Van der Waals were main acting forces. All the above methods can be widely used to investigate the interaction of peptide with nucleic acids, which contributes to design the structure of new and efficient drugs.

Keywords Trp-Arg · ct DNA · Interaction mechanisms · Spectroscopic · Molecular modeling

Introduction

The interactions of peptides or small molecules with Deoxyribonucleic acid (DNA) have been the focus of some recent research works in the scope of life science [1]. For the agents which bind to DNA, intercalation, groove binding and electrostatic binding are the three primary binding modes [2–4]. The results of various interactive modes studies have been used in designing new and efficient clinic drug molecules [4, 5].

In recent studies, many peptides have found wide application in therapeutics, in particular, anticancer agents for their biological activity [6, 7]. Arg-containing peptides play an essential roles in a number of biological processes in human body because of its positive charge, thus it is fundamental importance for understanding the character and reactivity of the complex formation of Arg-containing peptides, the properties of the side chain guanidinium [8–10].

In the present study, the interaction mode between the ctDNA and WR, which contains the simple structure of Arg-containing peptide, simultaneously, applying Trp as a fluorescence probe [11, 12], has been investigated by the application of multiple spectroscopic techniques and molecular modeling. This work can benefit further understanding of the binding mechanism of WR with DNA and comprehension Arg-containing peptides' pharmacological effects as well as the design on the structure of new and efficient drug molecules.

Materials and Methods

Reagents

We prepared a stock solution of WR (1×10^{-3} mol L-1) by dissolving 0.019 g of WR (a purity of at least 95 %) purchased from GL Biochem Inc. (Shanghai, China) in 50 mL of water. This solution was further diluted as required

Calf thymus DNA (Beijing Biodee Biotechnology Co., Ltd., China) was prepared by dissolving appropriate solid DNA in 50 mL calibrated flask. This solution was preserved

J. Lin · C. Gao · R. Liu
Shandong Key Laboratory of Water Pollution Control and Resource Reuse, School of Environmental Science and Engineering, China-America CRC for Environment & Health, Shandong University, Shandong Province, 27# Shanda South Road, Jinan 250100, People's Republic of China

C. Gao · R. Liu (✉)
School of Environmental Science and Engineering, Shandong University, Jinan 250100, People's Republic of China
e-mail: rutaoliu@sdu.edu.cn

at 0–4 °C and shaken gently as needed. The nucleotide concentration was 7.2×10^{-4} molL^{-1}, determined by the absorbance at 260 nm (ε_{260}=6600 L mol^{-1} cm^{-1}) [13].

A 0.1 mol/L Tris–HCl buffer (pH=7.4) was used to control pH. When preparing the reaction systems in 10 ml standard flasks, 1.0 ml of Tris-HCl was added. The concentration of NaCl stock solution was 1 mol L^{-1}, by dissolving 5.844 g of NaCl (Tianjin Damao Chemical Reagent Factory) into100 mL of water.

All the chemicals used were of analytical-reagent grade. All solutions were prepared using ultrapure water (resistivity of 18.25 MΩ cm).

Apparatus

UV–Vis absorption spectra in aqueous solution by using a quartz cell having 1.0 cm pathway were all recorded on a double beam Shimadzu UV-2450 spectrophotometer.

All fluorescence spectra were measured on F-4600 fluorescence spectrophotometer (Hitachi Japan) with 1.0 cm path length fluorescence cuvette. The excitation and emission slit widths were set at 10 nm and the scan rate at1200 nm min^{-1}. PMT voltage was fixed at 600 V.

The CD spectra were made on a J-810 Spectropolarimeter (Jasco, Tokyo, Japan) in a 1.0 mm path length quartz cuvette.

pH measurements was measured with a pHs-3C acidity meter (Peng shun, Shanghai, China).

Molecular Docking Studies

All docking studies were carried out with AutoDock 4.2. The crystal structure of DNA duplex was 5′-d (CGCGAA TTCGCG)2-3′, which was obtained from NIH genetic sequence database(MMDB ID: 48220). The structure of WR (Scheme 1) encoded in Gaussian 03W input files and further refined by performing density functional theory (DFT) optimizations.

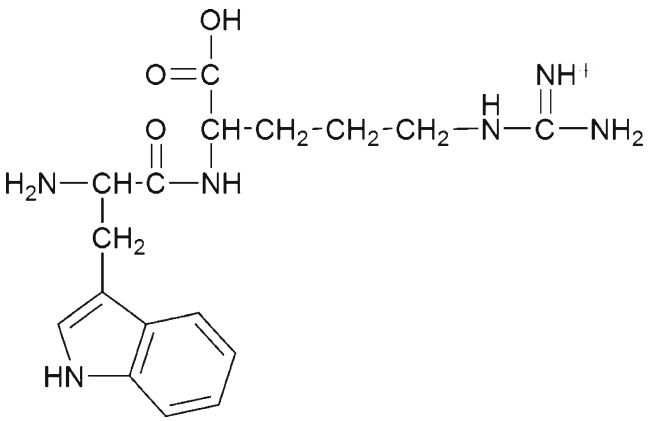

Scheme 1 The structure of WR

All the water molecules were removed, whereas Gasteiger charges and essential hydrogen atoms were added with the aid of AutoDock tools. The grid size was set to 60, 80 and110 along the X-, Y- and Z-axes, respectively. Furthermore, the ligand root of WR was detected and the rotatable bonds were defined.

The docking procedure was run and the binding site as well as the possible conformation of the complex generated from the reaction between DNA and WR was calculated.

Results and Discussion

UV Absorption Spectroscopy

UV Absorption Spectra of WR in the Presence of ctDNA

The binding of drugs to DNA has been characterized classically through hypochromism and hyperchromism in the absorption spectra [14–16]. When a drug molecule is intercalated between base pairs of nucleicacids, a red shift and hypochromism are observed of small molecules at the absorption maximum [17, 18].

Figure 1 shows that WR has absorption peaks at 220 and 280 nm. On addition of ctDNA a hypochromicity was observed without any band shift at both 220 nm and 280 nm. This result indicates that the binding mode is not the intercalative binding [19].

Considering that the binding of DNA has no significant effect on the UV absorption spectra of WR, which indicates that the binding mode of WR to DNA might be groove binding [20].

Moreover, the peak at 222 nm is assigned to the skeleton of WR, whereas the peak at 280 nm may be originated from

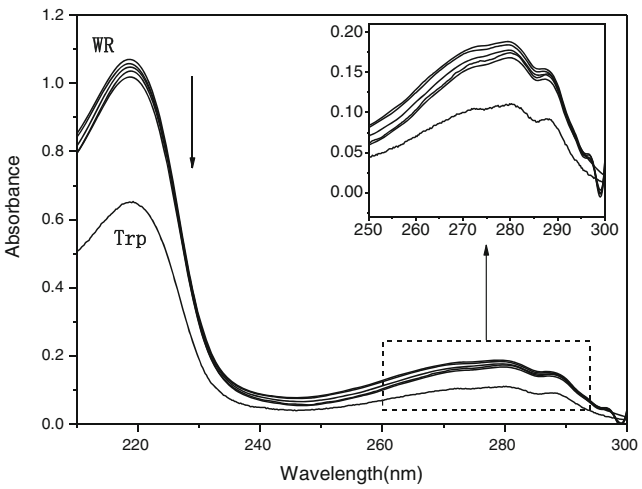

Fig. 1 UV-vis absorption spectra of WR in the absence and presence of ctDNA at different concentrations (pH=7.4, T=298 K). c(WR)=5×10^{-5} mol L^{-1}; c(Trp)=1×10^{-5} mol L^{-1}; c(DNA)/(×10^{-5} mol L^{-1}) *a*–*e*: 0, 2.16, 6.48, 8.64 and 10.8, respectively

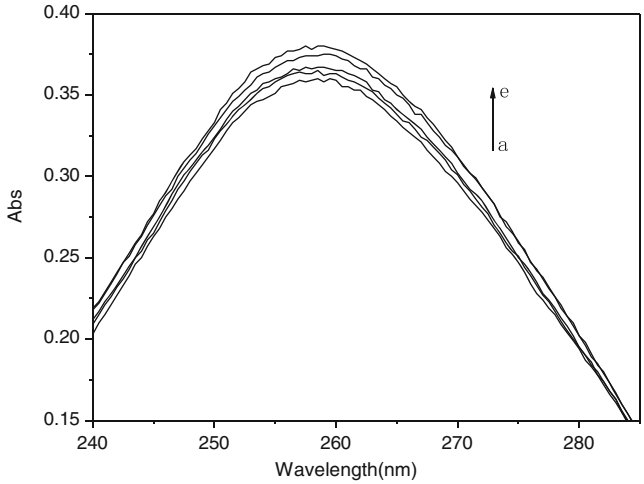

Fig. 2 UV-vis absorption spectra of ctDNA in the absence and presence of WR at different concentrations (pH=7.4, T=298 K). c(DNA)=7.2×10^{-5} mol L^{-1}; c(WR)/(×10^{-5} mol L^{-1}) *a–e*: 0, 1.50, 3.00, 4.50 and 6.00, respectively

the aromatic chromophore of WR. The latter shoulder peak at 288 nm corresponds to zero vibrational level of the electronic transition frequency [21].

UV Absorption Spectra of ctDNA in the Presence of WR

The application of absorption spectroscopy may give us useful information in DNA-binding [22]. Therefore, the effect of WR on the UV absorption spectra of DNA was also applied in this work. In the absorption spectrum, hyperchromism derives from damage to the DNA double-helix structure [23]. It can be seen from the experimental results shown in Fig. 2 a hypochromicity was observed without any band shift at 260 nm with the addition of ctDNA. This showed that the double helix is affected by the binding between WR and ctDNA.

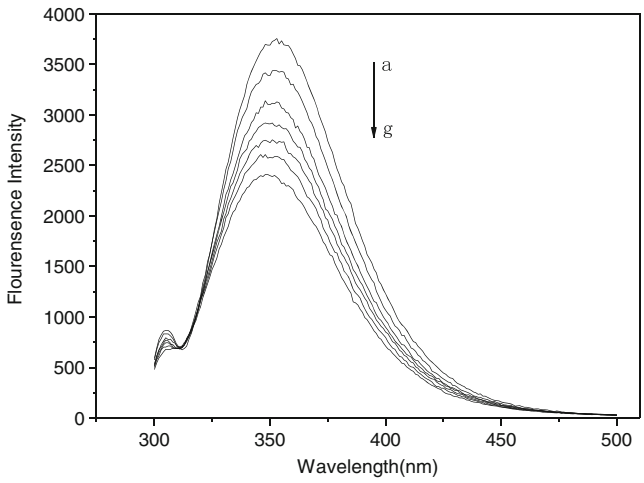

Fig. 3 Fluorescence spectra of WR in the absence and presence of ct DNA at different concentrations (pH=7.4, T=298 K). c(WR)=1×10^{-6} mol L^{-1}; c(DNA)/(×10^{-5} mol L^{-1}) (*a–g*): 0, 0.72, 1.44, 2.16, 2.88, 3.6 and 4.32, respectively

Measurement of Fluorescence Spectra

Fluorescence Measurements

The effect of DNA concentration on the fluorescence of WR was studied (Fig. 3). The maximum excitation wavelength is 278 nm and the maximum emission wavelength is 350 nm. Fluorescence intensity of WR decreases rapidly with the addition of DNA concentration.

As the structure of WR shows, the guanidine group is positively charged. Electrostatic binding may neutralize the negative charged phosphate groups of DNA [23], inducing distribution changes of electron, which may be

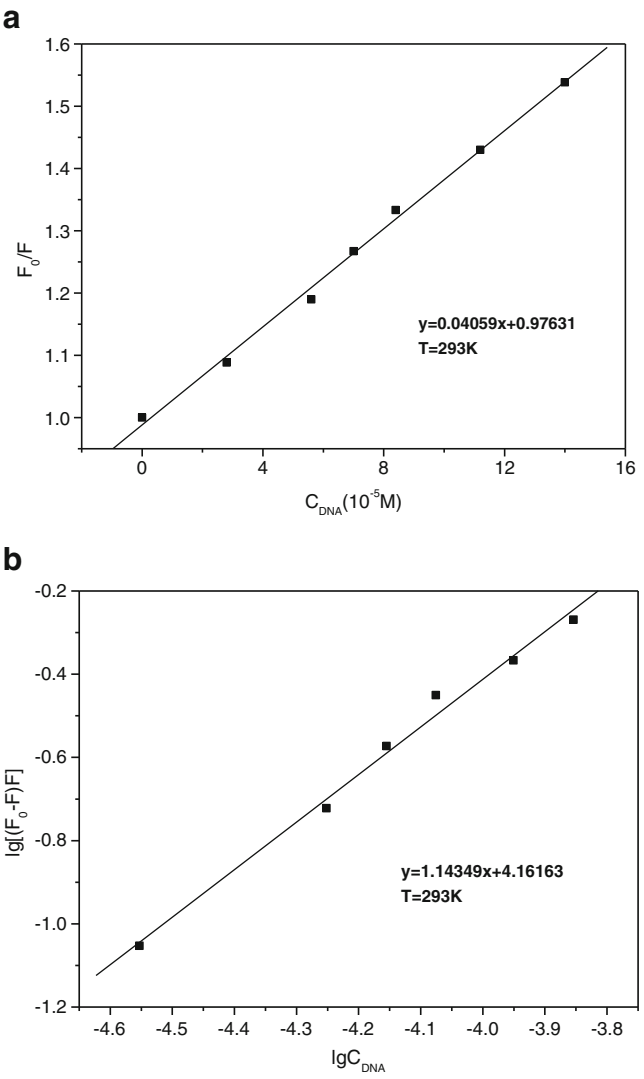

Fig. 4 **a** Stern–Volmer plot of the fluorescence quenching of WR with different concentrations of ctDNA. **b** Plot of lg((F_0-F)/F) versus lgC_{DNA} with the addition of various a mounts of ctDNA to WR

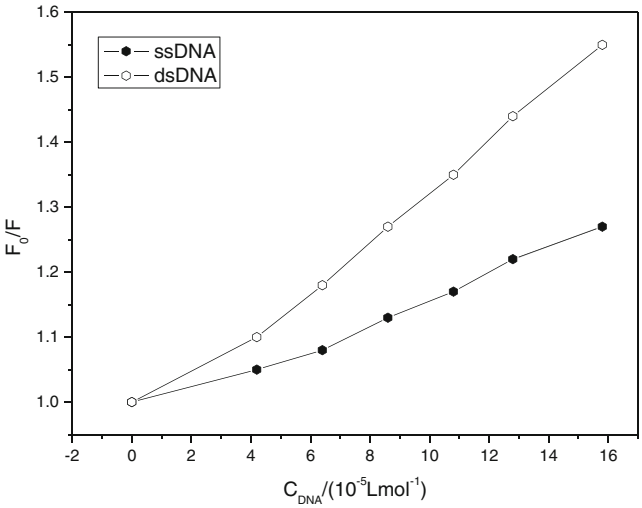

Fig. 5 Fluorescence quenching plots of WR in the presence of ssDNA and dsDNA at different concentrations, respectively (pH=7.4, T=298 K). c(WR)=1×10^{-6} mol L^{-1}

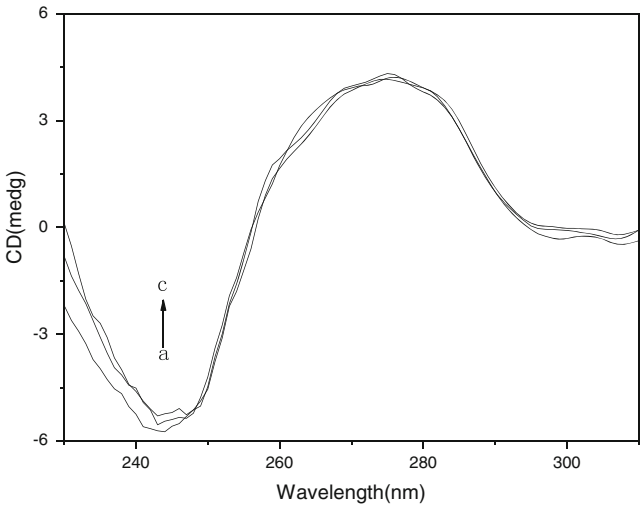

Fig. 7 CD spectra of DNA in the absence and presence of WR (pH=7.4, T=298 K). c(DNA)=7.2×10^{-5} mol L^{-1}; c(RAC)/(×10^{-5} mol L^{-1}): 0, 4 and 8, respectively

the most reasonable explanation for the fluorescence quenching [24]. Moreover, there is a H-bond formed between the attached amino-group near indole and DNA. Thus, the π-π conjugation decreased and the fluorescence quenching occurred [25].

Fluorescence Quenching Mechanisms

The interaction of small molecule with biological macromolecule can cause fluorescence quenching which was classified into static quenching and dynamic quenching [26]. Therefore, the fluorescence quenching of WR by DNA should be analyzed using the modified Stern-Volmer equation (Eq. (1)) [27],

$$F_0/F = 1 + Kq\tau_0[Q] = 1 + Ksv[Q] \quad (1)$$

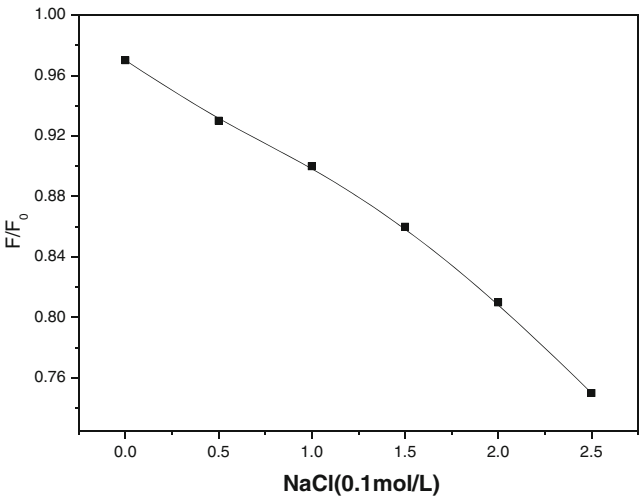

Fig. 6 Effects of ionic concentration on fluorescence spectra of WR (pH=7.4, T=298 K). c(DNA)=7.2×10^{-5} mol L^{-1}; c(WR)=1.0×10^{-6} mol L^{-1}

where F_0 and F are the fluorescence intensity of WR without and with DNA, respectively. [Q] is the concentration of the quencher, τ_0 is the lifetime of the fluorophore. Its value is about 10^{-8} s [28], Kq and Ksv are the bimolecular quenching constant and the Stern–Volmer quenching constant, respectively. The plots of lg[(F_0–F)/F] versus lg[Q] are shown in Fig. 4a. Kq was calculated from Ksv=Kqτ_0. For WR, the value of Kq is 4.1×10^{11} L mol^{-1} s^{-1}, which is far greater than 2.0×10^{10} L mol^{-1} s^{-1} (the maximum diffusion collision quenching rate constant). Thus, the fluorescence quenching mechanism of WR by DNA was revealed to be consequence of static quenching.

The binding constant (K) and the number of binding sites (n) can be obtained from Eq. (2) [29]

$$\lg[(F_0 - F)/F] = \lg K_A + n\lg[Q] \quad (2)$$

Where F_0, F and [Q] are the same as in Eq. (2), the linear relationship plots of F_0/F versus [Q] are shown in Fig. 4b.

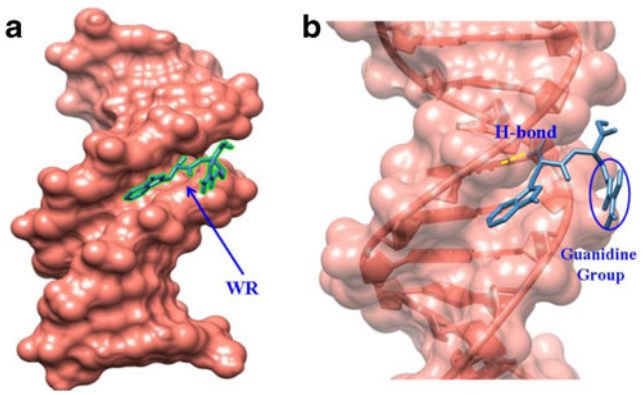

Fig. 8 Molecular modeling results of the WR and DpNA system. **a** Binding site of RAC to DNA. **b** Detailed illustration of the binding between WR and DNA

K_A is the binding constant and n is the hill coefficient. The calculated values of K_A is 1.4×10^4 $Lmol^{-1}$, which is lower than that of classical intercalative binding mode [14]. The groove-binding mode mentioned above can be verified again.

Effect of Native or Denatured DNA on Fluorescence Quenching

Further support for the groove binding of WR to DNA was obtained through the fluorescence quenching effect of single-stranded DNA (ssDNA) or double-stranded DNA (dsDNA) on WR. The dsDNA was converted into ssDNA by incubating the solution at 100 °C for 30 min followed by cooling in ice-water bath. The double-helix structure split into two string-like soft polynucleotide chains, which cause the difference in the fluorescence quenching [30]. In the absorption measurement, we can exclude the typical intercalation binding in the WR-DNA complex. If there was only an electrostatic mode, the quenching effect on the drug would not appear a significant change, for the ssDNA can still offer binding sites of the negatively charged phosphate groups [30, 31]. As can be seen from Fig. 5 that the quenching of denatured DNA is much smaller than the native DNA. Therefore, groove bindings are the major binding modes for the studied systems, the ssDNA will have less opportunity to bind the WR than dsDNA will do.

Effect of Ionic Strength on Fluorescence Quenching

The influence of ionic environment on the fluorescence quenching was assessed at various NaCl concentrations. Figure 6 represents the effect of ionic strength on the fluorescence quenching of WR caused by DNA. When the concentration of NaCl ranged from 0 to 0.25 mol L^{-1}, the corresponding fluorescence intensity continuously decreased. The above results can be explained as follows, DNA is an anionic polyelectrolyte, and Na^+ ions can neutralize the negatively charged phosphate backbone of DNA by electrostatic interaction [29, 32]. As a consequence, the double helix of DNA contracts longitudinally, which ultimately makes the groove of DNA narrower and deeper. This may be more prone to interact between WR and DNA. Finally, there are less free WR molecules in the solution, resulting in the decrease of fluorescence intensity [33]. These results provide further proof of the groove binding between WR and ctDNA.

Circular Dichroism Spectroscopy

Circular dichroism (CD) spectroscopy is useful in monitoring changes in DNA morphology during its interactions with exogenous substances [16, 34]. Therefore, CD can show if WR binding can alter the ctDNA conformation.

The ctDNA in the B conformation shows two conservative bands in the CD spectrum; a positive peak due to base stacking (275 nm) and a negative one owing to the helicity of DNA (245 nm) [35].

It can be seen from Fig. 7 that the intensities of the negative band decreased significantly (shifting to zero levels) accompanied by a slight red shift, whereas the change of the positive band is small with increasing [WR]/[DNA] ratio. The lack of new peak in CD spectra excludes the classic intercalation [36, 37]. Some investigators believed that this type of changes in the CD spectra may be characteristic of a shift from B-like DNA structure toward one with some contributions from an A-like conformation [38].

Such behavior suggests further that the double helix is destroyed, which is consistent with our experimental results of UV absorption spectra of ctDNA in the presence of WR; however, the binding modes do not significantly unwind DNA base pairs.

Molecular Modeling Studies

Docking method can provide the visual representation of the phenomenon of the interactions between the macromolecule and ligand, which can complement and substantiate the experimental results [39].

Compared with G-C regions, the narrower A-T regions is much more prone to generate a better fit of small molecules into the minor groove [33, 40]. Moreover, C-2 carbonyl oxygen of T or the N-3 nitrogen of A plays an important role in the formation of hydrogen bonding to the minor groove binders [41].

Structural analysis of Fig. 8(a) reveals a feature pertaining to the WR binding within the DNA minor groove. In our work, only one hydrogen bond between the N-3 nitrogen of A 18 on chain B (DA18B) and the N atom of the amino group on WR. In addition, electrostatic force forms between the phosphate groups on chain B (DT20B) and the Guanidine Group on WR. The above phenomenon was detailed in Fig. 8(b). The hydrogen bond as well as Van der Waals force proved to be dominant forces in the binding process by calculation of binding energy.

The optimized docked structures of WR–DNA predict a mixed mode of electrostatic and groove binding. This may be explained that the groove mode is the dominant mode and hence its manifestations are evident in experimental work.

Conclusions

In summary, two different modes of binding to DNA by WR have been found by spectroscopy and molecular modeling study.

The minor groove binding between WR and DNA proved by fluorescence spectroscopy, UV–visible absorption spectra, tests for the ability of WR binding with dsDNA and ssDNA, and the ionic effect in the fluorescence experiment, etc. The main forces to form WR–DNA complex are van der Waals forces and hydrogen bond. CD results showed deep conformational changes in the ctDNA double helix upon binding with the drug. This result is also supported by the docking studies. The molecular modeling results illustrated that WR tended to bind in the region of rich A–T base pairs through the hydrogen bond between A 18 and N atom of the amino group on WR. Furthermore, the calculated parameter shows that electrostatic binding also exists. Taken together we conclude that the binding model of WR and ct DNA obtained in this study is mixed-mode, and groove binding is probably the predominant one.

This study is very important for elucidating the molecular interaction mechanism and very useful for screening out or designing more efficient polypeptide drugs rationally. Further studies are in progress.

Acknowledgments The work is supported by NSFC (21277081), the Cultivation Fund of the Key Scientific and Technical Innovation Project, Ministry of Education of China (708058), and Independent innovation foundation of Shandong University natural science projects (2012DX002) are also acknowledged.

References

1. Zhao GC, Zhu JJ, Zhang JJ, Chen HY (1999) Voltammetric studies of the interaction of methylene blue with DNA by means of β-cyclodextrin. Anal Chim Acta 394(2–3):337–344
2. Erkkila KE, Odom DT, Barton JK (1999) Recognition and reaction of metallointercalators with DNA. Chem Rev 99(9):2777–2796
3. Zhang LZ, Tang GQ (2004) The binding properties of photosensitizer methylene blue to herring sperm DNA: a spectroscopic study. J Photochem Photobiol B 74(2–3):119–125
4. Dong C, Wei YX, Wei YL (2005) Study on the interaction between methylene violet and calf thymus DNA by molecular spectroscopy. J Photochem Photobiol A 174(1):15–22
5. Banitaba MH, Davarani SS, Mehdinia A, Mehdinia A (2011) Study of interactions between DNA and aflatoxin B1 using electrochemical and fluorescence methods. Anal Biochem 411(2):218–222
6. Torchilin VP, Lukyanov AN (2003) Peptide and protein drug delivery to and into tumors: challenges and solutions. Drug Discov Today 8(6):259–266
7. Zeng Q, Yin Q, Zhao Y (2005) The study on the interaction between seryl-histidine dipeptide and proteins by circular dichroism and molecular modeling. Bioorg Med Chem 13(7):2679–2689
8. Puspita WJ, Odani A, Yamauchi O (1999) Copper(II)–dipeptide complexes containing an acidic and a basic amino acid residue. Side chain effects on structures and stabilities. J Inorg Biochem 73(4):203–213
9. Kende AS, Dong HQ, Liu XW, Ebetino FH (2002) A useful synthesis of the Phe-Arg phosphinic acid dipeptide isostere. Tetrahedron Lett 43(28):4973–4976
10. Tan B, Yin YL, Kong XF, Li P, Li XL, Gao HJ, Li XG, Huang RL, Wu GY (2010) L-Arginine stimulates proliferation and prevents endotoxin-induced death of intestinal cells. Amino Acids 38(4):1227–1235
11. Iavarone AT, Patriksson A, van der Spoel D, Parks JH (2007) Fluorescence probe of Trp-cage protein conformation in solution and in gas phase. J Amer Chem Soc 129(21):6726–6735
12. Weber J, Wilke-Mounts S, Grell E, Senior AE (1994) Tryptophan fluorescence provides a direct probe of nucleotide binding in the noncatalytic sites of Escherichia coli F1-ATPase. J Biol Chem 269(15):11261–11268
13. Zou HY, Wu HL, Zhang Y, Li SF, Nie JF, Fu HY, Yu RQ (2009) Studying the interaction of pirarubicin with DNA and determining pirarubicin in human urine samples: combining excitation-emission fluorescence matrices with second-order calibration methods. J Fluoresc 19(6):955–966
14. Shi Y, Guo CL, Sun YJ, Liu ZL, Xu FG, Zhang Y, Wen ZW, Li Z (2011) Interaction between DNA and Microcystin-LR studied by spectra analysis and atomic force microscopy. Biomacromolecules 12(3):797–803
15. Taraszewska J, Piasecki AK (1987) Inclusion complexes of isomeric chloronitrobenzenes with α- and β-cyclodextrins studied by polarography: analysis of the possibilities of the method. J Electroanal Chem Interfac 226(1–2):137–146
16. Paramasivan S, Rujan I, Bolton PH (2007) Circular dichroism of quadruplex DNAs: applications to structure, cation effects and ligand binding. Methods 43(4):324–331
17. Wu HL, Li WY, He XW, Miao K, Liang H (2002) Spectral studies of the binding of lucigenin, a bisacridinium derivative, with double-helix. DNA Anal Bioanal Chem 373(3):163–168
18. Pansuriya PB, Patel MN (2008) Iron(III) complexes: preparation, characterization, antibacterial activity and DNA-binding. J Enzym Inhib 23(2):230–239
19. Zhang F, Du YX, Ye BF, Li P (2007) Study on the interaction between the chiral drug of propranolol and α1-acid glycoprotein by fluorescence spectrophotometry. J Photochem Photobiol B 86(3):246–251
20. Ling X, Zhong WY, Huang Q, Ni KY (2008) Spectroscopic studies on the interaction of pazufloxacin with calf thymus DNA. J Photochem Photobiol B 93(3):172–176
21. Middendorf TR, Aldrich RW, Baylor DA (2000) Modification of cyclic nucleotide–gated ion channels by ultraviolet light. J Gen Physiol 116(2):227–252
22. Tong CL, Xiang GH, Bai Y (2010) Interaction of paraquat with calf thymus DNA: a Terbium(III) luminescent probe and multispectral study. J Agric Food Chem 58(9):5257–5262
23. Sun YJ, Ji FY, Liu RT, Lin J, Xu QF, Gao CZ (2012) Interaction mechanism of 2-aminobenzothiazole with herring sperm DNA. J Lumin 132(2):507–512
24. Chai J, Wang JY, Xu QF, Hao F, Liu RT (2012) Multispectroscopic methods combined with molecular modeling dissect the interaction mechanisms of ractopamine and calf thymus DNA. Mol Biosyst 8(7):1902–1907
25. Tian LL, Zhang W, Yang B, Lu P, Zhang M, Lu D, Ma Y, Shen J (2005) Zinc(II)-induced color-tunable fluorescence emission in the π-conjugated polymers composed of the bipyridine unit: a way to get white-light emission. J Phys Chem B 109(15):6944–6947
26. Ding F, Liu W, Liu F (2009) A study of the interaction between malachite green and lysozyme by steady-state fluorescence. J Fluoresc 19(5):783–791
27. Cui FL, Yan YH, Zhang QZ, Qu GR, Du J, Yao XJ (2010) A study on the interaction between 5-Methyluridine and human serum albumin using fluorescence quenching method and molecular modeling. J Mol Model 16(2):255–262

28. Lakowicz JR, Weber G (1973) Quenching of fluorescence by oxygen. Probe for structural fluctuations in macromolecules. Biochem 12(21):4161–4170
29. Zhang GW, Hu X, Zhao N, Li WB, He L (2010) Studies on the interaction of aminocarb with calf thymus DNA by spectroscopic methods. Pestic Biochem Physiol 98(2):206–212
30. Li WY, Xu JG, He XW (2000) Characterization of the binding of methylene blue to DNA by spectroscopic methods. Anal Lett 33(12):2453–2464
31. Liu RT, Yang JH, Wu X (2002) Study of the interaction between nucleic acid and oxytetracycline–Eu3+ and its analytical application. J Lumin 96(2–4):201–209
32. Pratviel G, Bernadou J, Meunier B (1995) Carbon—hydrogen bonds of DNA sugar units as targets for chemical nucleases and drugs. Angew Chem Int Ed 34(7):746–769
33. Bi SY, Qiao CY, Song DQ, Tian Y, Gao DJ, Sun Y, Zhang HQ (2006) Study of interactions of flavonoids with DNA using acridine orange as a fluorescence probe. Sensors Actuators B 119(1):199–208
34. Chi ZX, Liu RT, Sun YJ, Wang MJ, Zhang PJ, Gao CZ (2010) Investigation on the toxic interaction of toluidine blue with calf thymus DNA. J Hazard Mater 175(1–3):274–278
35. Arjmand F, Sharma GC, Sayeed F, Muddassir M, Tabassum S (2011) De novo design of chiral organotin cancer drug candidates: validation of enantiopreferential binding to molecular target DNA and 5′-GMP by UV–visible, fluorescence, 1H and 31P NMR. J Photochem Photobiol B105(3):167–174
36. Sinha R, Islam MM, Bhadra K, Kumar GS, Banerjee A, Maiti M (2006) The binding of DNA intercalating and non-intercalating compounds to A-form and protonated form of poly(rC) · poly(rG): Spectroscopic and viscometric study. Bioorg Med Chem 14(3):800–814
37. Wang L, Liu RT, Teng Y (2011) Study on the toxic interactions of Ni2+ with DNA using neutral red dye as a fluorescence probe. J Lumin 131(4):705–709
38. Patra AK, Nethaji M, Chakravarty AR (2007) Synthesis, crystal structure, DNA binding and photo-induced DNA cleavage activity of (S-methyl-l-cysteine)copper(II) complexes of heterocyclic bases. J Inorg Biochem 101(2):233–244
39. Yang XL, Wang AH-J (1999) Structural studies of atom-specific anticancer drugs acting on DNA. Pharmacol Therapeut 83(3):181–215
40. Hawkins CA, Watson C, Yan YF, Gong B, Wemmer DE (2001) Structural analysis of the binding modes of minor groove ligands comprised of disubstituted benzenes. Nucleic Acids Res 9(4):936–942
41. Sahoo BK, Ghosh KS, Bera R, Dasgupta S (2008) Studies on the interaction of diacetylcurcumin with calf thymus-DNA. Chem Pys 351(1–3):163–169